

Radiative corrections to the Triple Higgs Coupling in the Inert Higgs Doublet Model

Abdesslam Arhrib^{1,2*}, Rachid Benbrik^{3,4†}, Jaouad El Falaki^{1‡}, Adil Jueid^{1§}

¹ *Département de Mathématiques, Faculté des Sciences et Techniques, Université Abdelmalek Essaadi, B. 416, Tangier, Morocco.*

² *Physics Division, National Center for Theoretical Sciences, Hsinchu 300, Taiwan.*

³ *Faculty of Polydisciplinaire de Safi, Sidi Bouzid B.P 4162, 46000 Safi, Morocco.*

⁴ *LPHEA, Faculty of Science Semlalia, Cadi Ayyad University, Marrakesh, Morocco.*

Abstract

We investigate the implication of the recent discovery of a Higgs-like particle in the first phase of the LHC Run 1 on the Inert Higgs Doublet Model (IHDM). The determination of the Higgs couplings to SM particles and its intrinsic properties will get improved during the new LHC Run 2 starting this year. The new LHC Run 2 would also shade some light on the triple Higgs coupling. Such measurement is very important in order to establish the details of the electroweak symmetry breaking mechanism. Given the importance of the Higgs couplings both at the LHC and e^+e^- Linear Collider machines, accurate theoretical predictions are required. We study the radiative corrections to the triple Higgs coupling hhh and to hZZ , hWW couplings in the context of the IHDM. By combining several theoretical and experimental constraints on parameter space, we show that extra particles might modify the triple Higgs coupling near threshold regions. Finally, we discuss the effect of these corrections on the double Higgs production signal at the e^+e^- LC and show that they can be rather important.

* Email: aarhrib@ictp.it

† Email: rbenbrik@ictp.it

‡ Email: jaouad.elfalaki@gmail.com

§ Email: ajueid@ictp.it

I. INTRODUCTION

The discovery of a new particle with a mass around 125-126 GeV in the search for the Standard Model (SM) Higgs boson [1] was announced simultaneously by the ATLAS and CMS collaborations in July 2012 [2–7]. Since then, more data has been taken and analyzed at the LHC. One of the primary goals of the Higgs groups at the LHC is now to study the properties of this new resonance and determine if it is indeed the state predicted by the SM.

With this new discovery, a program of precision measurement involving the Higgs boson has just started and will get improved with the new run of LHC and future e^+e^- Linear Collider (LC). In fact, the $7 \oplus 8$ TeV data allow the measurement of the Higgs couplings to gauge bosons and $\tau^+\tau^-$ with about 20-30% of precision while the Higgs couplings to $b\bar{b}$ and $t\bar{t}$ still suffer large uncertainties of about 40-50%. All these measurements will be improved with the new run of LHC at 13-14 TeV and the future e^+e^- LC.

In order to confirm that the discovered Higgs-like particle is the SM Higgs responsible for the electroweak symmetry breaking, we need to know all its couplings to SM particles with accurate precision and also measure the trilinear and quartic self-couplings of the Higgs in order to be able to reconstruct the scalar potential. In this regards, the LHC with its high luminosity option have also the capability of measuring the SM triple Higgs couplings through one of the following channels $gg \rightarrow hh \rightarrow b\bar{b}\gamma\gamma, b\bar{b}\tau^+\tau^-, b\bar{b}W^\pm W^{\mp*}$ [8, 9]. The e^+e^- LC, which will provide some high precision measurement of the Higgs mass and its properties such as couplings to SM particles and quantum numbers, would also be able to perform SM triple Higgs coupling through $e^+e^- \rightarrow Zhh$ (double Higgs-Strahlung) and $e^+e^- \rightarrow \nu_e\bar{\nu}_e hh$ (WW fusion) with more than 700 GeV center of mass energy with better precision [10]. In the double Higgs-Strahlung process Zhh the Z boson will be reconstructed from l^+l^- or $q\bar{q}$ pairs, while for the WW fusion process the two Higgs can be reconstructed from $b\bar{b}b\bar{b}$ or $b\bar{b}$ and W^+W^- .

The discovery of this Higgs-like particle resonance opens a new era in elementary particle physics and leads to several theoretical and phenomenological studies on Higgs physics both in the SM and beyond. One of the very simplest extension of SM is the IHDM proposed, more than three decade ago, by Deshpande and Ma [11] for electroweak symmetry breaking

purpose. Recently, the IHDM model has been very attractive because it provides a dark matter candidate [12, 13], generates tiny neutrino masses [14] and also solve the naturalness problem [15]. Phenomenology of IHDM have been extensively studied during last decade [13, 16, 17].

The aim of this paper is to study the effect of the one loop radiative corrections to the triple Higgs coupling hhh as well as hZZ coupling in the framework of the IHDM. We will also compute the well known SM radiative corrections to the triple Higgs coupling as check of our procedure. Once these effect are well studied, we then proceed to the evaluation of radiative corrections to the double Higgs Strahlung process $e^+e^- \rightarrow Zh h$. For this purpose, we will apply an on-shell renormalization scheme to evaluate these one-loop corrections. For the numerical evaluation, we will take into account all the theoretical and experimental constraints on the scalar sector of the Model.

The paper is organized as follow: in the second section we introduce the IHDM model and describe the theoretical and experimental constraints that the model is subject to. In the third section we introduce the on-shell renormalization scheme for the triple Higgs coupling hhh and hZZ in the IHDM and present our numerical results in the fourth section. Numerical analysis of the double Higgs-strahlung is presented in the fifth section. Our conclusion is given in the last section.

II. THE INERT HIGGS DOUBLET MODEL

A. The Model

The IHDM is one of the most simplest models for the scalar dark matter, a version of a two Higgs double model with an exact Z_2 symmetry. The SM scalar sector is extended by an inert scalar doublet H_2 which can provide a stable dark matter candidate. Under Z_2 symmetry all the SM particles are even while H_2 is odd and it could mix with the SM-like Higgs doublet. We shall use the following parameterization of the two doublets :

$$H_1 = \begin{pmatrix} G^\pm \\ \frac{1}{\sqrt{2}}(v + h + iG^0) \end{pmatrix}, \quad H_2 = \begin{pmatrix} H^\pm \\ \frac{1}{\sqrt{2}}(H^0 + iA^0) \end{pmatrix} \quad (1)$$

with G^0 and G^\pm are the Nambu-Goldstone bosons absorbed by the longitudinal component of W^\pm and Z^0 , respectively. v is the vacuum expectation value (VEV) of the SM Higgs H_1 . Within the IHDM the scalar doublet H_2 does not couple with the SM fermions and therefore the H_2 -fermions interaction are present only through mixing with H_1 . The most general renormalizable, gauge invariant and CP invariant potential is given by :

$$V = \mu_1^2 |H_1|^2 + \mu_2^2 |H_2|^2 + \lambda_1 |H_1|^4 + \lambda_2 |H_2|^4 + \lambda_3 |H_1|^2 |H_2|^2 + \lambda_4 |H_1^\dagger H_2|^2 + \frac{\lambda_5}{2} \left\{ (H_1^\dagger H_2)^2 + \text{h.c} \right\} \quad (2)$$

In the above potential there is no mixing terms like $\mu_{12}^2 (H_1^\dagger H_2 + \text{h.c})$ because of the unbroken Z_2 symmetry. By hermicity of the potential, all $\lambda_i, i = 1, \dots, 4$ parameters are real. The phase of λ_5 can be absorbed by a suitable redefinition of the fields H_1 and H_2 , therefore the scalar sector is CP conserving. After spontaneous symmetry breaking of $SU(2)_L \otimes U(1)_Y$ down to $U(1)_Q$, the spectrum of this potential will have five scalar particles: two CP even H^0 and h which will be identified as the SM Higgs boson, a CP odd A^0 and a pair of charged scalars H^\pm . Their masses are given by:

$$\begin{aligned} m_h^2 &= -2\mu_1^2 = 2\lambda_1 v^2 \\ m_{H^0}^2 &= \mu_2^2 + \lambda_L v^2 \\ m_{A^0}^2 &= \mu_2^2 + \lambda_S v^2 \\ m_{H^\pm}^2 &= \mu_2^2 + \frac{1}{2}\lambda_3 v^2 \end{aligned} \quad (3)$$

where $\lambda_{L,S}$ are defined as:

$$\lambda_{L,S} = \frac{1}{2}(\lambda_3 + \lambda_4 \pm \lambda_5) \quad (4)$$

This model involves 8 independent parameters: five λ , two μ_i and v . One parameter is eliminated by the minimization condition and the VEV is fixed by the W boson mass. Finally, we are left with six independent parameters which we choose as follow :

$$\{\mu_2^2, \lambda_2, m_h, m_{H^\pm}, m_{H^0}, m_{A^0}\} \quad (5)$$

B. Theoretical and Experimental Constraints

In order to have vacuum stability, the parameters of the potential need to satisfy the positivity conditions. Namely, the potential should be bounded from below in all the directions of the field space, i.e. should not go to negative infinity for large field values. We have this set of constraints :

$$\lambda_1 > 0 \quad , \quad \lambda_2 > 0 \quad , \quad \lambda_3 + 2\sqrt{\lambda_1\lambda_2} > 0 \quad \text{and} \quad \lambda_3 + \lambda_4 - |\lambda_5| > 2\sqrt{\lambda_1\lambda_2} \quad (6)$$

We ask that the perturbative unitarity is maintained in variety of scattering processes at high energy: scalar-scalar, scalar-vector, vector-vector. Using the equivalence theorem which replaces the W and Z bosons by the Goldstone bosons. We find a set of four matrices with entries are the quartic couplings, the diagonalization of these matrices gives us this set of eigenvalues [18]:

$$\begin{aligned} e_{1,2} &= \lambda_3 \pm \lambda_4 \quad , \quad e_{3,4} = \lambda_3 \pm \lambda_5 \\ e_{5,6} &= \lambda_3 + 2\lambda_4 \pm 3\lambda_5 \\ e_{7,8} &= -\lambda_1 - \lambda_2 \pm \sqrt{(\lambda_1 + \lambda_2)^2 + \lambda_4^2} \\ e_{9,10} &= -3\lambda_1 - 3\lambda_2 \pm \sqrt{9(\lambda_1 - \lambda_2)^2 + (2\lambda_3 + \lambda_4)^2} \\ e_{11,12} &= -\lambda_1 - \lambda_2 \pm \sqrt{(\lambda_1 - \lambda_2)^2 + \lambda_5^2} \end{aligned} \quad (7)$$

By requiring that $e_i \leq 8\pi$, we find the strongest constraint on $\lambda_{1,2}$ to be: $\lambda_{1,2} \leq \frac{4\pi}{3}$. We also require that the parameters of the scalar potential remains perturbative, i.e: $|\lambda_i| \leq 8\pi$.

In order to have an inert vacuum the following constraint should be satisfied [19]:

$$m_h^2, m_{H^\pm}^2, m_{H^0}^2, m_{A^0}^2 > 0 \quad \text{and} \quad v^2 > -\frac{\mu_2^2}{\sqrt{\lambda_1\lambda_2}} \quad (8)$$

The extra scalar particles affects quantum corrections to the W and Z bosons self energies. The corrections are parameterized by the oblique parameters, S , T and U [20] which are constrained from electroweak precision measurements. Taking the reference Higgs mass as $m_h = 125$ GeV and $m_t = 173$ GeV, the tolerated ranges are found at fixed $U=0$ [21]:

$$\Delta S = 0.06 \pm 0.09, \quad \text{and} \quad \Delta T = 0.10 \pm 0.07 \quad (9)$$

with correlated factor of +0.91. Where $\Delta S = S^{\text{IHDM}} - S^{\text{SM}}$ and $\Delta T = T^{\text{IHDM}} - T^{\text{SM}}$. The formulas for ΔS and ΔT in the IHDM can be found in Ref [15, 22].

Searches of scalar particles ¹ of the IHDM at colliders [23] is not directly performed yet. However, several studies [24–26] applied SUSY searches involving two, three or multiple leptons with missing transverse energy E_T^{miss} to the case of IHDM and set some limits on the dark Higgses. We choose in our analysis ² :

$$m_\Phi \geq 100 \text{ GeV} \quad \text{where } \Phi = H^\pm, H^0, A^0 \quad (10)$$

Finally, the magnitude of a possible Higgs boson signal at the LHC is characterized by the signal strength modifier, defined as $R_{\gamma\gamma}$ by :

$$R_{\gamma\gamma} = \frac{\sigma(pp \rightarrow h \rightarrow \gamma\gamma)^{\text{IHDM}}}{\sigma(pp \rightarrow h_{\text{SM}} \rightarrow \gamma\gamma)} = \frac{Br(h \rightarrow \gamma\gamma)^{\text{IHDM}}}{Br(h_{\text{SM}} \rightarrow \gamma\gamma)} \quad (11)$$

h_{SM} denotes a 125 GeV SM Higgs boson. In our analysis below, while we will show points which satisfy theoretical and experimental constraints from our scans, we will highlight the points for which $R_{\gamma\gamma}$ is consistent with the measured $\mu_{\gamma\gamma}$ at the LHC. The latest publicly available measurements read [27, 28]

$$\mu_{\gamma\gamma}^{\text{CMS}} = 1.13 \pm 0.24 \quad (12)$$

$$\mu_{\gamma\gamma}^{\text{ATLAS}} = 1.17 \pm 0.27 \quad (13)$$

III. RADIATIVE CORRECTIONS TO TRIPLE HIGGS COUPLINGS hhh AND hZZ

In this section we calculate the one-loop radiative corrections to the trilinear Higgs coupling hhh and hZZ in the SM and IHDM. The correction to those two couplings are part of the correction to double Higgs strahlung process $e^+e^- \rightarrow Zh h$ which we will discuss in

¹ these dark Higgses have the same signature like neutralinos and charginos of the Minimal Supersymmetric Standard Model (MSSM).

² if H or A is DM candidate then its mass could be as low as few GeV.

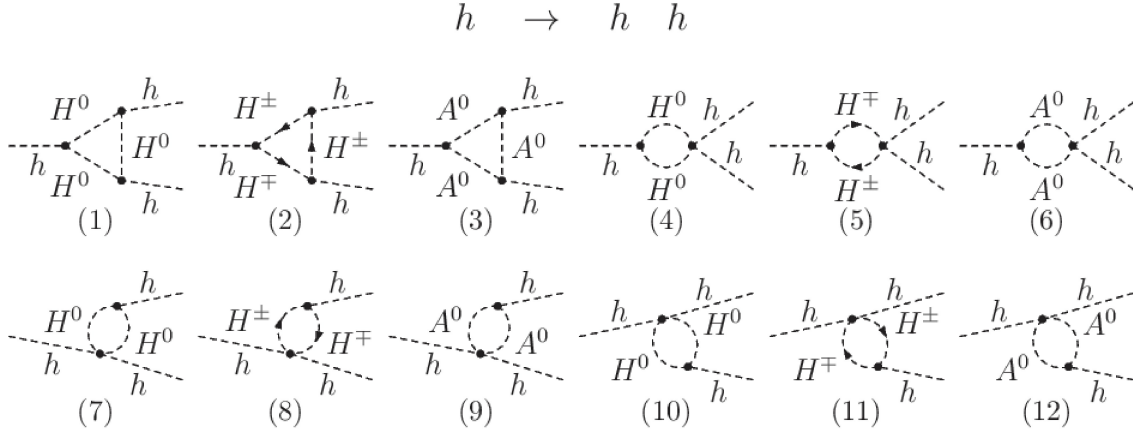


FIG. 1. One loop Feynman diagrams contributing to hhh in the IHDM. S stands for H^\pm, G^\pm, G^0 and $V = W^\pm$.

section V. Those couplings are given at the tree-level by:

$$\lambda_{hhh} = \frac{-3m_h^2}{v} \quad (14)$$

$$hZ_\mu Z_\nu = \frac{em_W}{s_W c_W^2} g_{\mu\nu} \quad (15)$$

As one can see, both couplings hhh and hZZ involve only SM parameters. Those couplings receive corrections from one-loop diagrams. The one-loop effects from the SM particles have been studied in [30–32] for hhh and in [29] for hZZ . These effects are dominated by the top quark loops which does not exceed 10% for hhh and 1.5% for hZZ .

New physics effects to hhh coupling have been analyzed in the context of the Two Higgs Doublet Model [30] and the MSSM [32]. It was found that these effects can enhance significantly this coupling in a wide range of parameter space. Furthermore, these corrections depend on the model and hence any deviation from the SM tree level relation (14) by more than 10% would be an evidence for the presence of new physics.

The coupling hZZ have been analyzed in the framework of the two Higgs doublet model [31] and it has been found that the effect is rather small 1% to 2%.

We have calculated the radiative corrections to the tree level triple Higgs coupling hhh and hZZ both in the SM and IHDM in the Feynman gauge including all the particles of the model in the loops. The Feynman diagrams from IHDM contributing to λ_{hhh} coupling are shown in Fig.(1).

The one-loop amplitude are calculated using dimensional regularization. The calculation was done with the help of FeynArts and FormCalc [33] packages. Numerical evaluation of the one-loop scalar integrals have been done with LoopTools [34]. We have checked both numerically and analytically the UV finiteness of the amplitudes.

In order to do that, we have considered hhh and hZZ at one-loop level:

i) for hhh , we considered the decay of an off-shell Higgs boson into a Higgs boson pairs $h^*(q) \rightarrow h(k_1)h(k_2)$ at the one-loop level. Where q , k_1 and k_2 are the 4-momenta of the three particles satisfying on shell conditions $k_1^2 = k_2^2 = m_h^2$ for final state Higgs pairs and an off shell condition $q^2 \neq m_h^2$ for the decaying Higgs.

ii) For hZZ , we follow ref [31] and write:

$$M_{hZZ}^{\mu\nu}(q^2 = m_h^2, k_1^2, k_2^2) = M_1^{hZZ} g^{\mu\nu} + M_2^{hZZ} \frac{k_1^\nu k_2^\mu}{m_Z^2} + M_3^{hZZ} i\epsilon^{\mu\nu\rho\sigma} \frac{k_{1\rho} k_{2\sigma}}{m_Z^2}, \quad (16)$$

where k_1 and k_2 are the momenta of outgoing Z bosons. We assume that the decaying Higgs and one of the Z boson are on-shell $q^2 = m_h^2$, $k_1^2 = m_Z^2$ while the other Z boson is off-shell $k_2^2 = (m_h - m_Z)^2$. Using power counting arguments, it is expected that M_1^{hZZ} receives the highest power contribution of the heavy fermions masses. Therefore, in what follow we will take into account only the M_1^{hZZ} form-factor to hZZ coupling.

Since we are dealing with a processes at the one-loop level, a systematic treatment of the UV divergences have to be considered. We will use the on-shell renormalization scheme in which the input parameters coincide with the physical masses and couplings [35]. In the on shell scheme, a redefinition of the fields and parameters is performed. This redefinition cast the Lagrangian into a bare Lagrangian and counter-term. The counter-terms are calculated by specific renormalization conditions which allow us to cancel the UV divergences of the diagrams with loops. Furthermore, since we have three Higgs as external particles and there is no mixing between the SM doublet H_1 and the inert doublet H_2 , we do not need to renormalize the particle content of the scalar potential of the IHDM. The tree level coupling hhh eq. (14) depends only on Higgs mass and the vev as in the SM, then the renormalization procedure will be the same as in the SM [35]. We redefine the SM fields and parameters as

follow:

$$\begin{aligned}
m_V^2 &\rightarrow m_V^2 + \delta m_V^2 \quad , \quad V = W^\pm, Z \\
m_h^2 &\rightarrow m_h^2 + \delta m_h^2 \\
s_W &\rightarrow s_W + \delta s_W \\
e &\rightarrow (1 + \delta Z_e)e \\
t &\rightarrow t + \delta t \\
W^\mu &\rightarrow Z_W^{1/2} W^\mu = \left(1 + \frac{1}{2} \delta Z_W\right) W^\mu \\
Z^\mu &\rightarrow \left(1 + \frac{1}{2} \delta Z_{ZZ}\right) Z^\mu + \frac{1}{2} \delta Z_{ZA} A^\mu \\
A^\mu &\rightarrow \left(1 + \frac{1}{2} \delta Z_{AA}\right) A^\mu + \frac{1}{2} \delta Z_{AZ} Z^\mu \\
h &\rightarrow Z_h^{1/2} h = \left(1 + \frac{1}{2} \delta Z_h\right) h
\end{aligned} \tag{17}$$

where $s_W = \sin \theta_W$ is the Weinberg angle and $t = v(\mu_1^2 - \lambda_1 v^2)$ is the tadpole which is zero at tree level once the minimization condition is used but will receives again finite radiative corrections at the one-loop level. To ensure that the VEV is the same in all orders of perturbation theory, it is well known that one need to renormalize the Higgs tadpole: i.e, all Higgs tadpole amplitudes T are absorbed into the counter-term δt . Thus, we put the first condition:

$$\hat{T} = \delta t + T = 0 \tag{18}$$

The mass counter-terms are fixed by the on shell conditions [35]:

$$\begin{aligned}
\text{Re} \hat{\Sigma}_T^{VV}(m_V^2) &= 0 \quad , \quad V = W, Z \\
\text{Re} \hat{\Sigma}_h(m_h^2) &= 0
\end{aligned} \tag{19}$$

The field renormalization constants are fixed by imposing that the residue of the two point Green functions to be equal to unity and the mixing γ - Z vanish for $k^2 = m_Z^2$. While the electric charge renormalization constant δZ_e is treated like in quantum electrodynamics and is fixed from the $e^+e^-\gamma$ vertex. The renormalized three point function $\hat{\Gamma}_{e^+e^-\gamma}^\mu$ satisfy at the Thomson limit:

$$\hat{\Gamma}_{e^+e^-\gamma}^\mu(\not{p}_1 = \not{p}_2 = m, q^2 = 0) = e$$

Furthermore, the counter-term δs_W can be obtained from the on-shell definition $s_W^2 = 1 - \frac{m_W^2}{m_Z^2}$ as a function of δm_W and δm_Z .

Inserting these redefinitions into the Lagrangian, we find the following counter term for hhh and hZZ [35]:

$$\delta\mathcal{L}_{hhh} = \frac{-3e^2}{2s_W} \frac{m_h^2}{m_W} \left(\delta Z_e - \frac{\delta s_W}{s_W} + \frac{\delta m_h^2}{m_h^2} + \frac{e}{2s_W} \frac{\delta t}{M_W m_h^2} - \frac{\delta m_W^2}{2m_W^2} + \frac{3}{2} \delta Z_h \right) h^3 \quad (20)$$

$$\delta\mathcal{L}_{hZZ} = \delta M_1 = \frac{em_W}{s_W c_W^2} \left(\delta Z_e + \frac{2s_W^2 - c_W^2}{c_W^2 s_W} \delta s_W + \frac{\delta m_W^2}{2m_W^2} + \frac{1}{2} \delta Z_H + \delta Z_Z \right) h Z^\mu Z^\nu \quad (21)$$

By adding the un-renormalized amplitude for hhh and hZZ to the above corresponding counter-terms, one find the renormalized amplitudes

$$\begin{aligned} \hat{\Gamma}_{hhh}(q^2, m_h^2, m_h^2) &= \Gamma_{hhh}^{1-loop}(q^2, m_h^2, m_h^2) + \delta\mathcal{L}_{hhh} \\ \hat{\Gamma}_{hZZ}(m_h^2, m_Z^2, (m_h - m_Z)^2) &= M_{1hZZ}^{tree} + M_{1hZZ}^{1-loop} + \delta\mathcal{L}_{hZZ} \end{aligned} \quad (22)$$

which becomes UV finite. For our numerical illustrations, we define the following ratios:

$$\Delta\Gamma_{hhh} = \frac{\text{Re}(\tilde{\Gamma}_{hhh}(q^2))}{\lambda_{hhh}} \quad (23)$$

$$\Delta\Gamma_{hZZ} = \frac{\hat{\Gamma}_{hZZ}^{IDM} - \hat{\Gamma}_{hZZ}^{SM}}{M_{1hZZ}^{tree}} = \frac{M_1^{IDM} - M_1^{SM-tree}}{M_1^{SM-tree}} \quad (24)$$

Where $\hat{\Gamma}_{hhh}$ is the renormalized vertex.

IV. NUMERICAL RESULTS

A. SM case

In our numerical analysis, the parameters are chosen as follow :

$$m_t = 173.5 \text{ GeV} \quad , \quad m_W = 80.3996 \text{ GeV} \quad , \quad m_Z = 91.1875 \text{ GeV} \quad , \quad \alpha = \frac{1}{127.934}$$

and the on-shell definition of the Weinberg angle: $\sin^2 \theta_W = 1 - \frac{m_W^2}{m_Z^2}$.

In the SM, the dominant contribution to $\Delta\Gamma_{hhh}(SM)$ comes from top quark loops [30, 32]. We have computed the top contribution and shown that it is in perfect agreement with

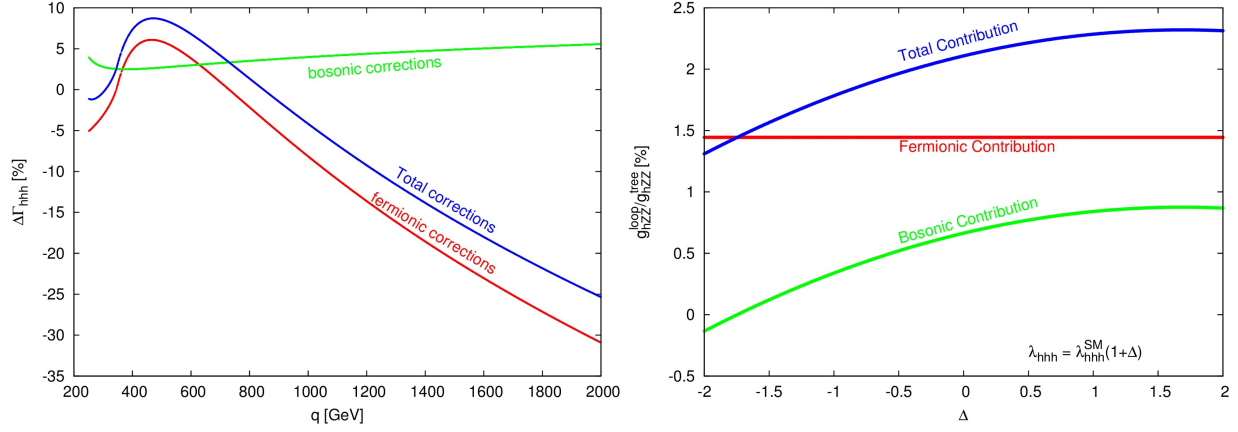


FIG. 2. (Left) $\Delta\Gamma_{hhh}(SM)$ as a function of h^* momentum q . (Right) $\Delta\Gamma_{hZZ}(SM)$ as a function of Δ which is the size of deviation from SM triple coupling $\lambda_{hhh} = \lambda_{hhh}^{SM}(1 + \Delta)$. It is shown: the fermionic contribution, the bosonic one as well as the total contribution.

Ref. [30]. We have also isolated and evaluated the other SM contributions without fermions. It turn out that this bosonic contribution is of the order of 5% for large q .

In Fig. (2)(left), it is illustrated that the top contribution to $\Delta\Gamma_{hhh}(SM)$ is negative before the opening of $h^* \rightarrow t\bar{t}$ threshold and also for $q \geq 700$ GeV. It is clear that for large q , $\Delta\Gamma_{hhh}(SM)$ is dominated by top-quark contribution.

In Fig. (2)(right), we show the radiative corrections to hZZ in the SM. We present separately the fermionic corrections which are dominated by the top contributions and the bosonic contributions. The total corrections to hZZ is of the order of 2%. In this plot, we also shift the triple Higgs SM coupling λ_{hhh}^{SM} by $\lambda_{hhh}^{SM}(1 + \Delta)$, where Δ represent any deviation from SM coupling. As one can see from the green line, the sensitivity to Δ is rather mild. Due to custodial symmetry, it is expected that hWW coupling will enjoy similar effect as hZZ and that is why we illustrate only the case of hZZ .

B. IHDM case

Here, we will show our numerical analysis for the triple coupling of the Higgs in the IHDM taking into account: unitarity, perturbativity, false vacuum as well as vacuum stability constraints described above. We take the mass of the SM Higgs $m_h = 125$ GeV and the masses of the inert particles to be degenerate, i.e : $m_{H^\pm} = m_{H^0} = m_{A^0} = m_\Phi$. For the other

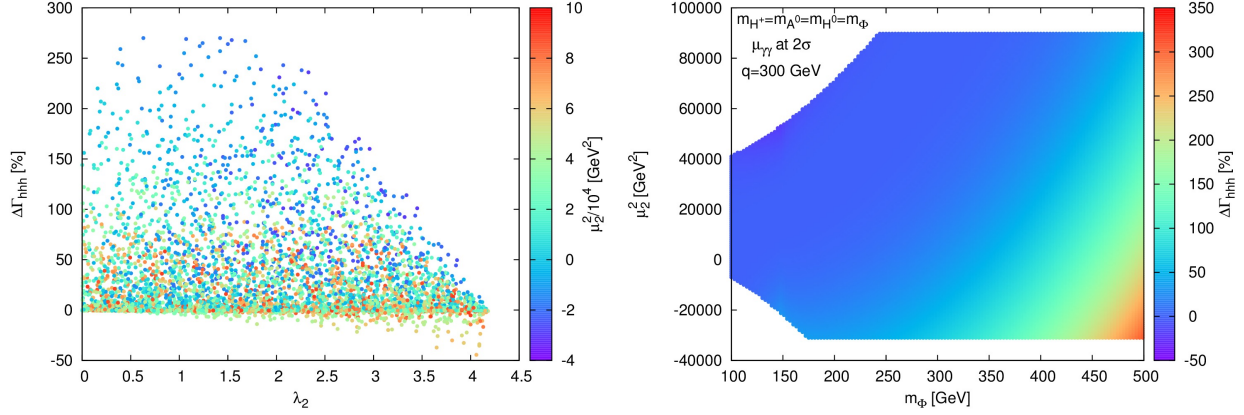


FIG. 3. Left: $\Delta\Gamma_{hhh}(IHDM)$ as a function of λ_2 . Right: Scatter plot for $\Delta\Gamma_{hhh}$ in the plan (m_Φ, μ_2^2) for $q = 300$ GeV, Left column show the size of the corrections. m_Φ and μ_2^2 are scanned as in eq. (25).

parameters, we perform the following scan:

$$\begin{aligned}
 100 \text{ GeV} &\leq m_\Phi \leq 500 \text{ GeV} \\
 -25 \times 10^5 (\text{GeV})^2 &\leq \mu_2^2 \leq 9 \times 10^5 (\text{GeV})^2 \\
 0 &< \lambda_2 \leq \frac{4\pi}{3}
 \end{aligned} \tag{25}$$

We plot in Fig. (3)(left) the relative corrections to the triple coupling as a function of λ_2 . The theoretical constraints put a limit on λ_2 parameter which is $\lambda_2 \leq \frac{4\pi}{3}$. One can see from Fig. 3 that the corrections are maximized for $\lambda_2 \leq 2$ and decrease for $\lambda_2 > 2$. In our following analysis, We will take $\lambda_2 = 2$ in order to maximize the effect from λ_2 .

In Fig. (3)(right), we plot the relative corrections to the triple coupling hhh in the plane (m_Φ, μ_2^2) for a fixed $q = 300$ GeV and $\lambda_2 = 2$. One can see that the corrections are very important in a large part of the parameter space with an enhancement up to 280% for large values of m_Φ and negative μ_2^2 . Furthermore, these corrections are increasing, for a fixed value of m_Φ , while μ_2^2 is decreasing. The maximum of the corrections is reached for $\mu_2^2 \approx -30000 (\text{GeV})^2$. Moderate or very small corrections which can be in the range $[-50, 50]\%$ are also possible for large area of parameter space with low $m_\Phi \leq 300$ GeV and any positive μ_2^2 . It is also important to note that LHC constraint from diphoton at the 2σ level exclude light charged Higgs $100 < m_{H^\pm} < 175$ GeV and negative μ_2^2 : left-down corner of the scatter plot. In Fig. 4 we show the relative corrections $\Delta\Gamma_{hhh}(IHDM)$ as a function of the momentum of

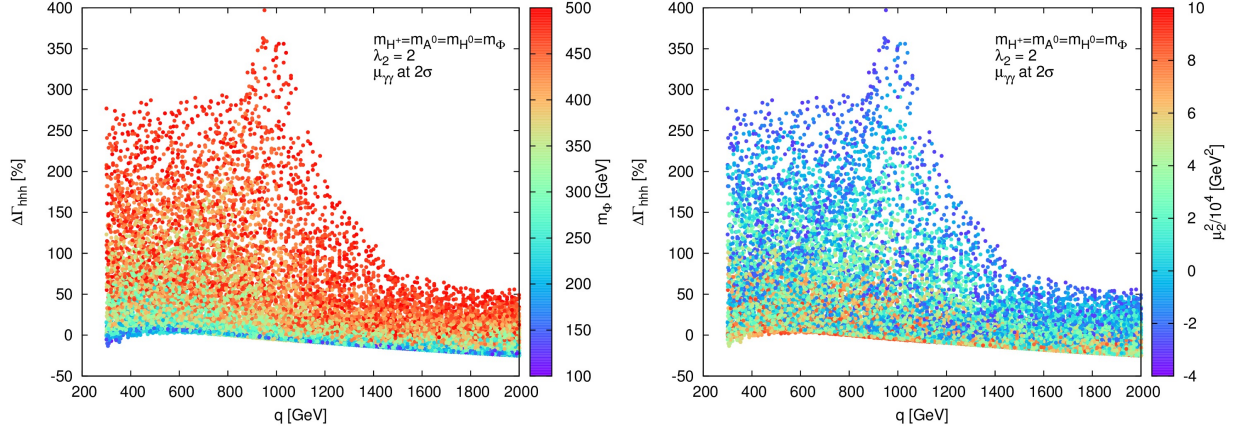


FIG. 4. $\Delta\Gamma_{hhh}(IHDM)$ as a function of q and where m_Φ and μ_2^2 are scanned as in eq. (25). The left column shows the values of m_Φ (left panel) and μ_2^2 (right panel)

the off-shell decaying Higgs q and for m_Φ and μ_2^2 as shown in eq. (25). It is clear that for low $100 < m_\Phi < 200$ GeV, the corrections are small like in the SM case except at the threshold regions where we have $\Delta\Gamma_{hhh} \sim -40\%$ due to the opening of $h^* \rightarrow \Phi\Phi$. For large m_Φ these corrections could be extremely large exceeding 100% in large area of parameter space. The corrections are amplified by the opening of the threshold channel $h^* \rightarrow \Phi\Phi$. This is visible on the left panel of Fig. 4 where we can see a kink for $q = 1000$ GeV which correspond to threshold effect $h^* \rightarrow \Phi\Phi$ with $m_\Phi \approx 500$ GeV. As it is shown, negative values for μ_2^2 gives large corrections to the triple Higgs coupling. This is because in our assumption of taking degenerate Higgses $m_{H^0} = m_{A^0} = m_{H^\pm} = m_\Phi$ one can show that $\lambda_4 = \lambda_5 = 0$, $\lambda_3 = \frac{2}{v^2}(m_{H^\pm}^2 - \mu_2^2)$ and therefore the triple coupling are given by

$$\begin{aligned}
 hHH &= \lambda_L v = \frac{2}{v}(m_\Phi^2 - \mu_2^2) \\
 hAA &= \lambda_A v = \frac{2}{v}(m_\Phi^2 - \mu_2^2) \\
 hH^+H^- &= \lambda_3 v = \frac{2}{v}(m_\Phi^2 - \mu_2^2)
 \end{aligned} \tag{26}$$

It is clear that those couplings gets stronger for negative μ_2^2 . We now examine the effect of the radiative corrections on the triple coupling in the case where the invisible decay $h \rightarrow HH$ is open. This is illustrated in Fig. 5(left) and right. In Fig. 5(left) we impose both $|\lambda_L| < 0.02$ required by dark matter constraints as well as best fit limit on the invisible branching ratio $Br(h \rightarrow invisible) \leq 10\%$ (left) and $Br(h \rightarrow invisible) \leq 20\%$ (right) [36]. It is clear from left panel that with dark matter constraint, the size of the corrections and

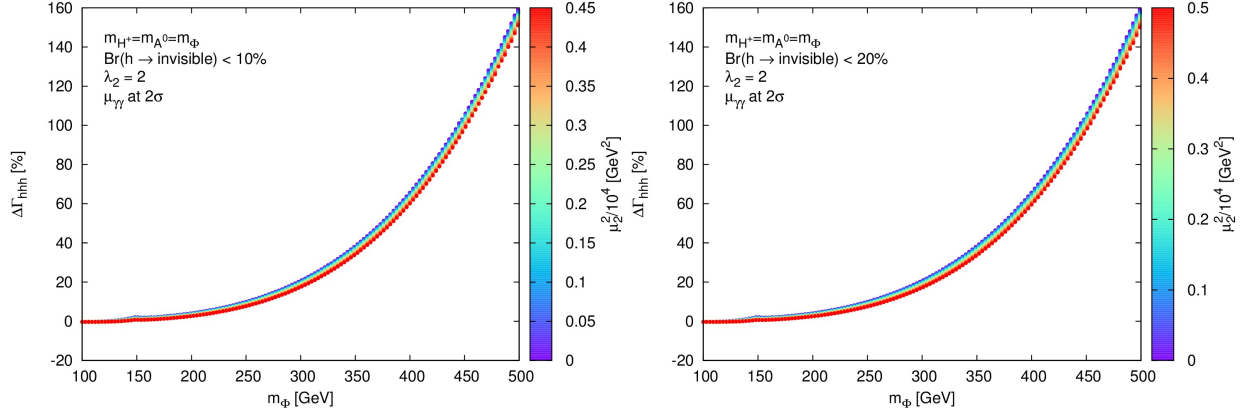


FIG. 5. $\Delta\Gamma_{hhh}$ as a function of m_Φ for $q = 300$ GeV with μ_2^2 in the range given by the Eq. (25) and invisible decay of the Higgs ($h \rightarrow HH$) is open. Left panel with dark matter constraint which restrict $|\lambda_L|$ to be in the range $|\lambda_L| < 0.02$. Right panel without dark matter constraint.

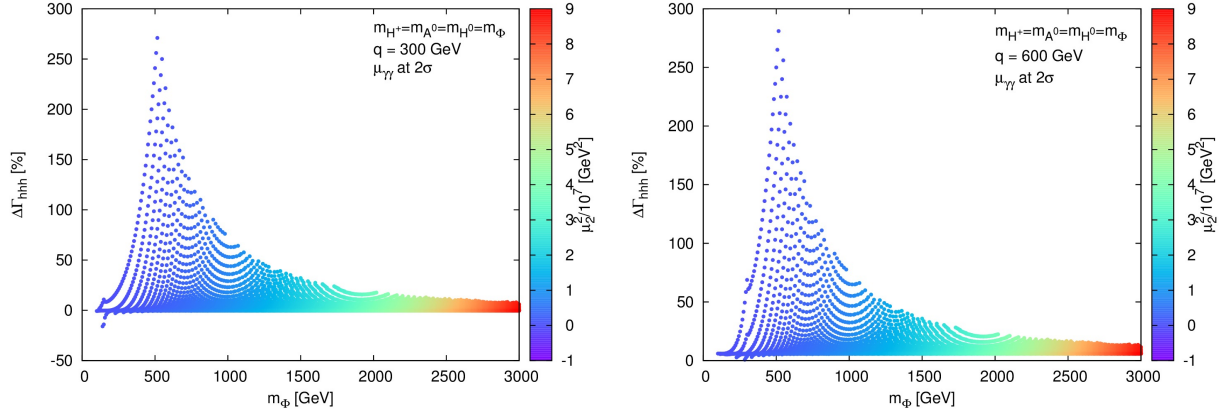


FIG. 6. Left: $\Delta\Gamma_{hhh}(IHDM)$ as a function of m_Φ for fixed $\lambda_2 = 2$ and $q = 300$ GeV (left), while $q = 600$ GeV in the right. Left column show the range of μ_2^2 .

the range of μ_2^2 are smaller than in the previous case where the invisible decay was closed. The large corrections observed for high m_Φ are mainly due to the charged Higgs loops.

In order to exhibit the decoupling behavior on the triple Higgs coupling, We increase both the range of μ_2^2 to be $[-10^6, 10^7] \text{ GeV}^2$ as well as the range of $m_\Phi \in [0.1, 3] \text{ TeV}$. We see that the decoupling effect occurs when appropriate combinations of the involved parameters are taken large compared to the electroweak scale. We find that $\Delta\Gamma_{hhh}$ reaches its maximum for $m_\Phi \approx 500$ GeV and decrease to SM value for large m_Φ .

In Fig. (7) we illustrate the IHDM effect on hZZ coupling. Similar to the triple Higgs coupling, we fix $\lambda_2 = 2$ and scan over μ_2^2 and $m_\Phi = m_H = m_A = m_{H\pm}$ as in eq. (25). In Fig. (7)(left) we show scatter plot for $\Delta\Gamma_{hZZ}$ in the plan (μ_2^2, m_Φ) , contrarily to the triple

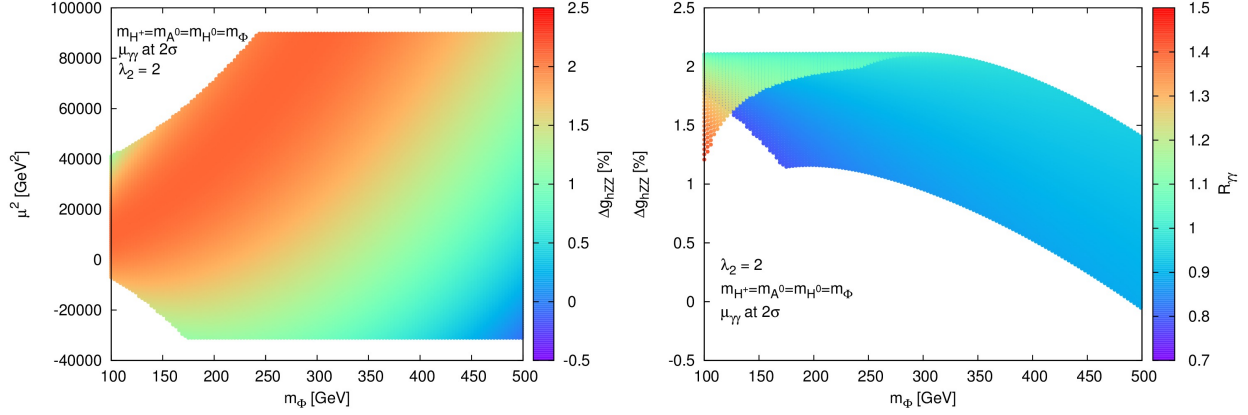


FIG. 7. Left: Scatter plot for $\Delta\Gamma_{hZZ}$ in the plan (m_Φ, μ_2^2) with $\lambda_2 = 2$, left column represent the size of the corrections. Right: $\Delta\Gamma_{hZZ}$ as function of m_Φ with μ_2^2 in the same range as in the left panel. Left column show the size of $R_{\gamma\gamma}$.

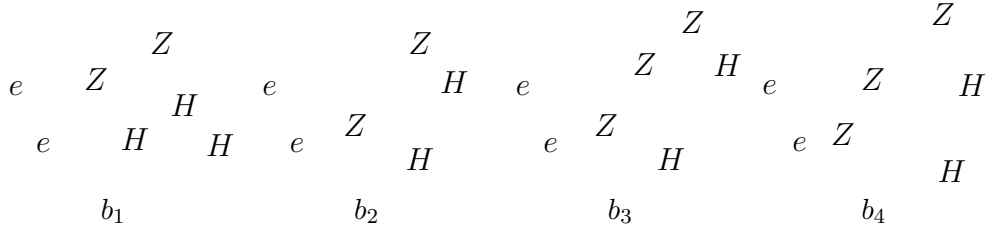


FIG. 8. Feynman diagrams contributing to $e^+e^- \rightarrow ZhZ$ at the tree level in SM

coupling hhh the effect are rather small of the same size as in the SM case. In Fig. (7)(right) we show the corrections to hZZ coupling and also the value of the corresponding $R_{\gamma\gamma}$ within 2σ range.

V. RADIATIVE CORRECTIONS TO $e^+e^- \rightarrow hhZ$ IN THE IHDM

A. $e^+e^- \rightarrow hhZ$ in SM

At e^+e^- LC, the triple Higgs coupling can be probed by double Higgsstrahlung process $e^+e^- \rightarrow hhZ$ depicted in Fig. (8) and WW fusion process $e^+e^- \rightarrow WW^*\nu\bar{\nu} \rightarrow hh\nu\bar{\nu}$. Note that $e^+e^- \rightarrow hhZ$ process arise in s -channel only and hence its cross section can be probed more efficiently at low energies above the threshold (typically between 350 GeV and 500 GeV). While, at high energies, for $\sqrt{s} \gtrsim 700$ GeV, the trilinear Higgs-coupling is

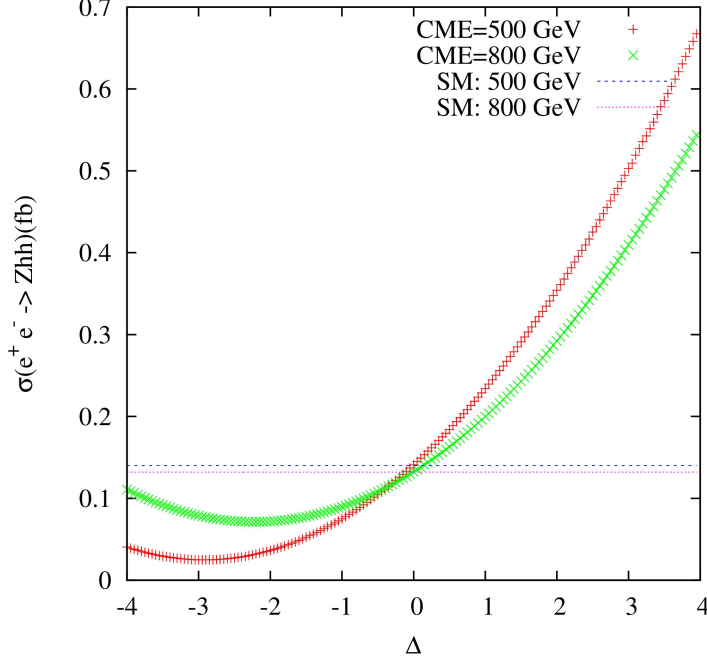


FIG. 9. Cross section of $e^+e^- \rightarrow Zhh$ as a function of Δ where $\lambda_{hhh} = \lambda_{hhh}^{SM}(1+\Delta)$ for $\sqrt{s} = 500, 800$ GeV.

better probed through the process $e^+e^- \rightarrow \nu\bar{\nu}hh$ assuming the SM. In Fig. (8) we show the Feynman diagrams contributing to $e^+e^- \rightarrow hhZ$. When extracting the triple Higgs coupling hhh from this process only diagram Fig. (8)(b_1) is concerned, the other diagrams $b_{2,3,4}$ are considered as a background.

We illustrate in Fig. (8) the tree level cross section for $e^+e^- \rightarrow hhZ$ as a function of Δ for center of mass energy 500 GeV and 800 GeV, where Δ is the shift of the SM triple Higgs coupling $\lambda_{hhh} = \lambda_{hhh}^{SM}(1 + \Delta)$. It is clear that for $\Delta > 0$ the cross section is enhanced while for $\Delta < 0$ the cross section is reduced with respect to SM value.

B. One-loop Corrections to $e^+e^- \rightarrow Zhh$

We study in this section the effects of the one-loop radiative corrections to the Higgs tri-linear self-coupling calculated in the previous section on the double Higgs-Strahlung process

via Z boson exchange. In the context of the SM, the $\mathcal{O}(\alpha)$ electroweak corrections have been studied in [37] and it was found that these corrections are of the order 10%. However, these loop effects can be very large in beyond SM enhancing the total cross section by about 2 orders of magnitude in particular in models with extended Higgs sector. As outlined above, at the tree level, $e^+e^- \rightarrow hhZ$ have four diagrams as depicted in Fig. (8). Only the first diagram contribute to the signal while the others are considered as a background. In our analysis, we include one-loop correction only to the triple Higgs coupling hhh which is expected to give sizeable contribution. Only this correction contribute to the signal. Therefore, we did not include corrections to the initial state vertex e^+e^-Z , to the self energies of Z - Z and $\gamma - Z$ mixing, to the hZZ coupling and also we did not include the initial state radiation. In fact these corrections are well known in the SM and are not expected to deviate that much in the IHDM as we already show in the previous section for hZZ coupling. Moreover, we will not include corrections to $e^+e^- \rightarrow hhZ$ coming from boxes and pentagon diagrams. The one-loop amplitude can be written as follow:

$$\mathcal{M} = \mathcal{M}_{\text{tree}} + \mathcal{M}_{\text{loop}} \quad (27)$$

The squared amplitude at the one-loop level is then :

$$|\mathcal{M}|^2 = |\mathcal{M}_{\text{tree}}|^2 + 2\text{Re}\{\mathcal{M}_{\text{tree}}^* \mathcal{M}_{\text{loop}}\} + \mathcal{O}(\alpha^2) \quad (28)$$

Thus, the cross section is written as:

$$\sigma = \frac{1}{(2\pi)^2} \int \prod_{k=1}^3 \frac{d^3\mathbf{p}_k}{2E_k} \delta^{(4)}(q_1 + q_2 - p_1 - p_2 - p_3) \sum_{\text{spin, pola.}} |\mathcal{M}|^2 \quad (29)$$

where q_1 and q_2 are the four momentum of the incoming electron and positron, p_1, p_2 and p_3 are the four momentum of the outgoing particles, and the factor $\frac{1}{(2\pi)^2}$ arises from the flux of the initial particles.

For our studies, we define the ratio $\Delta\sigma$ by :

$$\Delta\sigma = \frac{\sigma_{\text{total}} - \sigma_{\text{tree}}}{\sigma_{\text{tree}}} = \frac{\sigma_{\text{loop}}}{\sigma_{\text{tree}}} \quad (30)$$

Where $\sigma_{\text{total}} = \sigma_{\text{tree}} + \sigma_{\text{loop}}$. This ratio measure the relative correction of the IHDM to the cross section with respect to the tree level result.

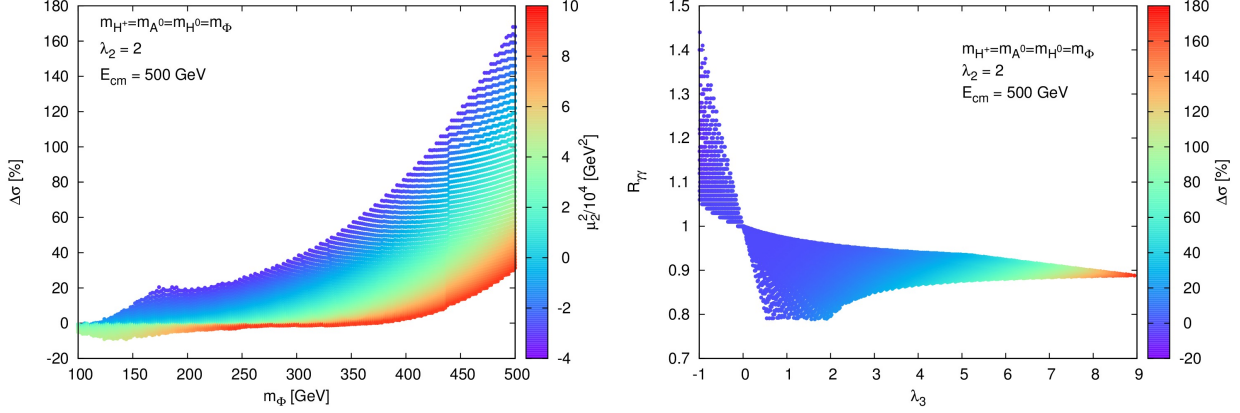


FIG. 10. (left): $\Delta\sigma$ as a function of m_Φ for $\sqrt{s} = 500$ GeV μ_2^2 values are shown in the right column, (right) $R_{\gamma\gamma}$ as a function of λ_3 and the right column shows $\Delta\sigma$ in % .

As stated before, in our analysis we will take into account the theoretical and experimental constraints discussed in the second section assuming the parameters to rely in the range given by eq. (25). The phase space and evaluation of the one-loop squared amplitude has been performed with FormCalc [33] with the help of LoopTools to evaluate numerically the one-loop scalar integrals. We have used the same on-shell renormalization scheme explained in the previous section.

In Fig. 10, we have plotted the ratio $\Delta\sigma$ versus m_Φ for center of mass energy $\sqrt{s} = 500$ GeV. We assume again that: $\lambda_2 = 2$, the dark Higgses to be degenerate $m_H = m_A = m_{H^\pm} = m_\Phi$ and perform a scan over μ_2^2 and m_Φ . From this plot one can see that the corrections can reach 160% for high dark Higgs masses $m_\Phi \approx 500$ GeV and are negative for low dark Higgs masses $100 \text{ GeV} \leq m_\Phi \leq 270$ GeV depending on the value of μ_2^2 . One can see that the suppression of the total cross section can reach -15% for $m_\Phi = 140$ GeV while the enhancement is predominant in most part of the parameter space.

To understand this, let us remind first that in large area of parameter space the correction to the triple Higgs coupling $\Delta\Gamma_{hhh}$ is positive (see section IV Fig. (3)). Moreover, according to the plot Fig. (9), if this correction is positive this lead to an enhancement of the total cross section and vice-versa.

This explain that in most of the case, the corrections to the cross section are positive and confirm that the behavior of the $\Delta\sigma$ is consistent with our analysis concerning the trilinear Higgs self coupling in the IHDM. We stress that the enhancement of $\Delta\sigma$ is observed in a large part of the parameter space and can exceed 100% only in the high mass region

$m_\Phi \geq 400$ GeV for $\mu_2^2 < 0$.

We plot in Fig. 10(right) the ratio $R_{\gamma\gamma}$ as a function of λ_3 and showing the relative corrections in the left column. For small values of $-1 < \lambda_3 < 2$ (low m_Φ) the corrections are quite small. For $\lambda_3 > 4$ (high m_Φ), $\Delta\sigma$ becomes more important and exceed 100%, this region corresponds to $R_{\gamma\gamma} \approx 0.9 \pm 0.02$. Note that our results concerning $R_{\gamma\gamma}$ are in agreement with the results of [22].

VI. CONCLUSION

We have computed the radiative corrections to triple Higgs coupling hhh , hZZ coupling as well as $e^+e^- \rightarrow Zhh$ in the framework of inert Higgs doublet model taking into account theoretical and experimental constraint on the parameter space of the model. The calculation was done in the Feynman gauge using dimensional regularization in the on-shell scheme. In the SM it is known that the top contribution to hhh coupling is of the order 10%, we found that the bosonic contribution is somehow significant and goes up to 5%. In the IHDM, we found that the total radiative corrections to the triple Higgs coupling could be substantial exceeding 100% for heavy dark Higgs masses m_H, m_A and m_{H^\pm} . We also show that the corrections to hhh are decoupling for large m_Φ and large μ_2^2 . In the case of hZZ coupling the effect is rather mild and do not exceed 2.5%. We also evaluate radiative corrections to the double Higgs strahlung process $e^+e^- \rightarrow Zhh$ by looking only to the correction to the diagram that contribute to the signal i.e the triple coupling hhh . We have shown that the correction are also very important. In general, the size of the loop effects, typically large, makes their proper inclusion in phenomenological analyses for future e^+e^- LC indispensable.

ACKNOWLEDGMENTS

A.A would like to thank NCTS for financial support where part of this work has been done. This work was supported by the Moroccan Ministry of Higher Education and Scientific Research MESRSFC and CNRST: "Projet dans les domaines prioritaires de la recherche scientifique et du développement technologique": PPR/2015/6. A.J would like to thank ICTP-Trieste for financial support during his stay where part of this work has been done.

APPENDIX

The Triple Higgs Coupling in the IHDM : Analytical Results

In this appendix, we present the analytical expression of the Higgs triple coupling at the one-loop order with the contribution of the inert scalars only. We use the Feynman diagrammatic method. The Feynman diagrams contributing to this process are shown in Fig. 1. By using the dimensional regularization, the amplitude is given by:

$$\begin{aligned}
\Gamma_{hhh}^{loop}(q^2, m_\Phi^2) = & \frac{\lambda_3^2 m_W s_W}{8e\pi^2} \left(B_0(q^2, m_{H^\pm}^2, m_{H^\pm}^2) + 2B_0(m_h^2, m_{H^\pm}^2, m_{H^\pm}^2) \right. \\
& + \frac{2\lambda_3 m_W^2 s_W^2}{\pi\alpha} C_0(q^2, m_h^2, m_h^2, m_{H^\pm}^2, m_{H^\pm}^2, m_{H^\pm}^2) \Big) \\
& + \frac{(\lambda_3 + \lambda_4 + \lambda_5)^2 m_W s_W}{16e\pi^2} \left(B_0(q^2, m_{H^0}^2, m_{H^0}^2) + 2B_0(m_h^2, m_{H^0}^2, m_{H^0}^2) \right. \\
& \times \frac{2(\lambda_3 + \lambda_4 + \lambda_5) m_W^2 s_W^2}{\pi\alpha} C_0(q^2, m_h^2, m_h^2, m_{H^0}^2, m_{H^0}^2, m_{H^0}^2) \Big) \\
& + \frac{(\lambda_3 + \lambda_4 - \lambda_5)^2 m_W s_W}{16e\pi^2} \left(B_0(q^2, m_{A^0}^2, m_{A^0}^2) + 2B_0(m_h^2, m_{A^0}^2, m_{A^0}^2) \right. \\
& \times \frac{2(\lambda_3 + \lambda_4 - \lambda_5) m_W^2 s_W^2}{\pi\alpha} C_0(q^2, m_h^2, m_h^2, m_{A^0}^2, m_{A^0}^2, m_{A^0}^2) \Big)
\end{aligned} \tag{31}$$

Where B_0 and C_0 are the Passarino-Veltman functions [38, 39].

Following the on-shell renormalization scheme, there are six renormalization constants to compute : $\delta m_h^2, \delta m_W^2, \delta m_Z^2, \delta t, \delta Z_e, \delta Z_h$ and δs_W . δZ_{AA} and δZ_{ZA} are the field renormalization constant for the photon and $Z - \gamma$ mixing respectively and are given by :

$$\delta Z_{AA} = \frac{\alpha}{\pi} \frac{\partial}{\partial p^2} B_{00}(p^2, m_{H^\pm}^2, m_{H^\pm}^2) \Big|_{p^2=0}, \quad \delta Z_{ZA} = \frac{\alpha(1 - 2s_W^2)}{2m_Z^2 c_W \pi} \left(-A_0(m_{H^\pm}^2) + 2B_{00}(0, m_{H^\pm}^2, m_{H^\pm}^2) \right) \tag{32}$$

The electric charge renormalization constant as well as the renormalization constants for the W and Z masses are given by:

$$\delta Z_e = -\frac{1}{2} \left(\delta Z_{AA} - \frac{s_W}{c_W} \delta Z_{ZA} \right), \tag{33}$$

$$\delta m_W^2 = \frac{\alpha}{16\pi s_W^2} \left(2A_0(m_{H^\pm}^2) + A_0(m_{A^0}^2) + A_0(m_{H^0}^2) + 4B_{00}(m_W^2, m_{H^\pm}^2, m_{H^0}^2) \right) \tag{34}$$

$$\delta m_Z^2 = -\frac{\alpha}{16\pi s_W^2 c_W^2} \left(-A_0(m_{A^0}^2) - A_0(m_{H^0}^2) - 2(1 - 2s_W^2)^2 A_0(m_{H^\pm}^2) + 4B_{00}(m_Z^2, m_{H^0}^2, m_{A^0}^2) \right. \\ \left. + 4(1 - 2s_W^2)^2 B_{00}(m_Z^2, m_{H^\pm}^2, m_{H^\pm}^2) \right) \quad (35)$$

The counter term δs_W , corresponding to the Weinberg mixing angle, is determined from the tree level relation $s_W^2 = 1 - m_W^2/m_Z^2$. δs_W is given by :

$$\delta s_W = \frac{-c_W^2}{2s_W} \left(\frac{\delta m_W^2}{m_W^2} - \frac{\delta m_Z^2}{m_Z^2} \right) \quad (36)$$

The counter-terms for the Higgs mass, Higgs field and the tadpole are given by :

$$\delta m_h^2 = \frac{1}{32\pi} \left(2\lambda_3 A_0(m_{H^\pm}^2) + (\lambda_3 + \lambda_4 + \lambda_5) A_0(m_{H^0}^2) + (\lambda_3 + \lambda_4 - \lambda_5) A_0(m_{A^0}^2) \right) \\ + \frac{m_W^2 s_W^2}{32\alpha\pi^3} \left(2\lambda_3^2 B_0(m_h^2, m_{H^\pm}^2, m_{H^\pm}^2) + (\lambda_3 + \lambda_4 + \lambda_5)^2 B_0(m_h^2, m_{H^0}^2, m_{H^0}^2) \right. \\ \left. + (\lambda_3 + \lambda_4 - \lambda_5)^2 B_0(m_h^2, m_{A^0}^2, m_{A^0}^2) \right) \quad (37)$$

$$\delta Z_h = \frac{m_W^2 s_W^2}{32\alpha\pi^3} \left(2\lambda_3^2 \frac{\partial}{\partial p^2} B_0(p^2, m_{H^\pm}^2, m_{H^\pm}^2) + (\lambda_3 + \lambda_4 + \lambda_5)^2 \frac{\partial}{\partial p^2} B_0(p^2, m_{H^0}^2, m_{H^0}^2) \right. \\ \left. + (\lambda_3 + \lambda_4 - \lambda_5)^2 \frac{\partial}{\partial p^2} B_0(p^2, m_{A^0}^2, m_{A^0}^2) \right) \Big|_{p^2=m_h^2} \quad (38)$$

$$\delta t = -\frac{m_W s_W}{16e\pi^2} \frac{1}{32\pi} \left(2\lambda_3 A_0(m_{H^\pm}^2) + (\lambda_3 + \lambda_4 + \lambda_5) A_0(m_{H^0}^2) + (\lambda_3 + \lambda_4 - \lambda_5) A_0(m_{A^0}^2) \right) \quad (39)$$

The expression for the triple Higgs coupling counter term is given in the third section eq. (20).

The renormalized triple Higgs coupling is given by :

$$\tilde{\Gamma}_{hhh}^{loop} = \Gamma_{hhh}^{loop} + \delta\Gamma_{hhh}^{loop}$$

We have checked that the renormalized amplitude is UV-finite and furthermore independent of the renormalization scale μ . We derive an approximate formula for $\tilde{\Gamma}_{hhh}^{loop}$. In the limit

$m_\phi = m_H = m_{A^0} = m_{H^\pm}$ and find a good agreement with full expression.

$$\begin{aligned}
\tilde{\Gamma}_{hhh}^{loop}(q^2, m_h^2, m_\phi^2) \approx & \frac{1}{8\alpha e \pi^3 q^2} \left[3\alpha \pi q^2 m_W s_W (2\lambda_3^2 + 2\lambda_3 \lambda_4 + \lambda_4^2 + \lambda_5^2) \left(x_1 \log\left(\frac{-1+x_1}{x_1}\right) + x_2 \log\left(\frac{-1+x_2}{x_2}\right) \right) \right. \\
& + \left. (2\lambda_3^3 + 3\lambda_3^2 \lambda_4 + 3\lambda_3 \lambda_4^2 + \lambda_4^3 + 3(\lambda_3 + \lambda_4)\lambda_5^2) m_W^2 s_W^2 \log^2\left(-\frac{q^2}{m_\phi^2}\right) \right] \\
& + \frac{x_1 x_2}{64\alpha m_W^3 m_Z^2 \pi^3 s_W^5 (x_1 - x_2)} \left((2\lambda_3^2 + 2\lambda_3 \lambda_4 + \lambda_4^2 + \lambda_5^2) (15em_W^4 m_Z^2) \right. \\
& + 4e\alpha^2 m_h^2 \pi^2 \left(m_Z^2 (m_h^2 - 2m_W^2 + m_Z^2) (-1 + 2s_W^2) + m_\phi^2 (-2m_Z^2 + m_W^2 (1 + (c_W^2 - s_W^2)^2) \right. \\
& + \left. \left. 4m_Z^2 s_W^2) \right) \right) \\
& \times \left((-1 + x_2) \log\left(\frac{-1+x_2}{x_2}\right) + (1 - x_1) \log\left(\frac{-1+x_1}{x_1}\right) \right) \\
& + \frac{x_1 x_2}{64m_W^3 \pi s_W^5 (x_1 - x_2)} \left(\alpha e m_h^2 (-2m_Z^2 + m_W^2 (3 + (c_W^2 - s_W^2)^2 - 4s_W^2) \right. \\
& + \left. 4m_Z^2 s_W^2 + m_h^2 (-2 + 4s_W^2) \right) \\
& \times \left(x_1 \log\left(\frac{-1+x_2}{x_2}\right) - x_2 \log\left(\frac{-1+x_1}{x_1}\right) \right) \\
& + \frac{\alpha^2 m_h^2 m_Z^2 \pi^2}{16em_W^3 m_Z^2 \pi^2 s_W^5} \left[-2m_Z^2 + m_W^2 (3 + (c_W^2 - s_W^2)^2 - 4s_W^2) + 4m_Z^2 s_W^2 + m_h^2 (-2 + 4s_W^2) \right] \\
& \times \left(x_1^3 \log\left(\frac{-1+x_1}{x_1}\right) - x_2^3 \log\left(\frac{-1+x_2}{x_2}\right) \right)
\end{aligned}$$

where $x_{1,2}$ are given by:

$$x_{1,2} = \frac{1 \mp \sqrt{1 - 4m_\phi^2/q^2}}{2} \quad (40)$$

-
- [1] F. Englert and R. Brout, Phys. Rev. Lett. **13** (1964) 321. P. W. Higgs, Phys. Rev. Lett. **13** (1964) 508. P. W. Higgs, Phys. Lett. **12** (1964) 132. P. W. Higgs, Phys. Rev. **145** (1966) 1156.
- [2] G. Aad *et al.* [ATLAS Collaboration], Phys. Lett. B **716**, 1 (2012) [arXiv:1207.7214 [hep-ex]].

- [3] G. Aad *et al.* [ATLAS Collaboration], "Evidence for Higgs Boson Decays to the $\tau^+\tau^-$ Final State with the ATLAS Detector", ATLAS-CONF-2013-108, November 2013
- [4] G. Aad *et al.* [ATLAS Collaboration], "Search for the bb decay of the Standard Model Higgs boson in associated W/ZH production with the ATLAS detector" ATLAS-CONF-2013-079, July 2013
- [5] S. Chatrchyan *et al.* [CMS Collaboration], Phys. Lett. B **716**, 30 (2012) [arXiv:1207.7235 [hep-ex]].
- [6] S. Chatrchyan *et al.* [CMS Collaboration], Phys. Rev. D **89**, 012003 (2014) [arXiv:1310.3687 [hep-ex]].
- [7] S. Chatrchyan *et al.* [CMS Collaboration], JHEP **1405**, 104 (2014) [arXiv:1401.5041 [hep-ex]].
- [8] E. W. N. Glover and J. J. van der Bij, Nucl. Phys. B 309, 282 (1988); C. T. Lu, J. Chang, K. Cheung and J. S. Lee, arXiv:1505.00957 [hep-ph]. T. Plehn, M. Spira and P. M. Zerwas, Nucl. Phys. B 479, 46 (1996) [Erratum-ibid. B 531, 655 (1998)]. J. Baglio, A. Djouadi, R. Gräber, M. M. Mühlleitner, J. Quevillon and M. Spira, JHEP 1304, 151 (2013). U. Baur, T. Plehn and D. L. Rainwater, Phys. Rev. D 69, 053004 (2004).
- [9] A. Djouadi, W. Kilian, M. Muhlleitner and P. M. Zerwas, Eur. Phys. J. C **10**, 45 (1999) [hep-ph/9904287]. M. J. Dolan, C. Englert and M. Spannowsky, JHEP **1210**, 112 (2012). A. Papaefstathiou, L. L. Yang and J. Zurita, Phys. Rev. D **87**, 011301 (2013). A. Ahriche, A. Arhrib and S. Nasri, Phys. Lett. B **743**, 279 (2015) [arXiv:1407.5283 [hep-ph]]. A. Arhrib, R. Benbrik, C. H. Chen, R. Guedes and R. Santos, the LHC," JHEP **0908**, 035 (2009) [arXiv:0906.0387 [hep-ph]].
- [10] D. M. Asner *et al.*, arXiv:1310.0763 [hep-ph]. A. Djouadi, W. Kilian, M. Muhlleitner and P. M. Zerwas, Eur. Phys. J. C **10**, 27 (1999) [hep-ph/9903229]. F. Borzumati and E. Kato, arXiv:1407.2133 [physics.pop-ph]. J. Tian *et al.* [ILD Collaboration], PoS EPS **-HEP2013**, 316 (2013) [arXiv:1311.6528 [hep-ph]].
- [11] N. G. Deshpande and E. Ma, Phys. Rev. D **18**, 2574 (1978).
- [12] M. Gustafsson, E. Lundstrom, L. Bergstrom and J. Edsjo, Phys. Rev. Lett. **99**, 041301 (2007) [astro-ph/0703512 [ASTRO-PH]]; T. Hambye and M. H. G. Tytgat, Phys. Lett. B **659**, 651 (2008) [arXiv:0707.0633 [hep-ph]]; P. Agrawal, E. M. Dolle and C. A. Krenke, Phys. Rev. D **79**, 015015 (2009) [arXiv:0811.1798 [hep-ph]]; E. Nezri, M. H. G. Tytgat and G. Vertongen, JCAP **0904**, 014 (2009) [arXiv:0901.2556 [hep-ph]]; E. M. Dolle and S. Su, Phys. Rev. D **80**,

- 055012 (2009) [arXiv:0906.1609 [hep-ph]];
- [13] A. Arhrib, Y. L. S. Tsai, Q. Yuan and T. C. Yuan, JCAP **1406**, 030 (2014) [arXiv:1310.0358 [hep-ph]].
 - [14] E. Ma, Phys. Rev. D **73**, 077301 (2006) [hep-ph/0601225]. S. Andreas, M. H. G. Tytgat and Q. Swillens, JCAP **0904**, 004 (2009) [arXiv:0901.1750 [hep-ph]];
 - [15] R. Barbieri, L. J. Hall and V. S. Rychkov, Phys. Rev. D **74**, 015007 (2006) [hep-ph/0603188].
 - [16] A. Arhrib, R. Benbrik and T. C. Yuan, Eur. Phys. J. C **74**, 2892 (2014) [arXiv:1401.6698 [hep-ph]].
 - [17] A. Goudelis, B. Herrmann and O. Stl, JHEP **1309**, 106 (2013) [arXiv:1303.3010 [hep-ph]].
 - [18] A. G. Akeroyd, A. Arhrib and E. M. Naimi, Phys. Lett. B **490**, 119 (2000) [arXiv:hep-ph/0006035].
 - [19] I. F. Ginzburg, K. A. Kanishev, M. Krawczyk and D. Sokolowska, Phys. Rev. D **82**, 123533 (2010) [arXiv:1009.4593 [hep-ph]].
 - [20] M. E. Peskin and T. Takeuchi, Phys. Rev. D **46** (1992) 381.
 - [21] M. Baak *et al.* [Gfitter Group Collaboration], Eur. Phys. J. C **74** (2014) 3046 [arXiv:1407.3792 [hep-ph]].
 - [22] A. Arhrib, R. Benbrik and N. Gaur, Phys. Rev. D **85**, 095021 (2012) [arXiv:1201.2644 [hep-ph]].
 - [23] G. Belanger, B. Dumont, A. Goudelis, B. Herrmann, S. Kraml and D. Sengupta, Phys. Rev. D **91**, no. 11, 115011 (2015) [arXiv:1503.07367 [hep-ph]].
 - [24] E. Dolle, X. Miao, S. Su and B. Thomas, Phys. Rev. D **81**, 035003 (2010) [arXiv:0909.3094 [hep-ph]].
 - [25] X. Miao, S. Su and B. Thomas, Phys. Rev. D **82**, 035009 (2010) [arXiv:1005.0090 [hep-ph]].
 - [26] M. Gustafsson, S. Rydbeck, L. Lopez-Honorez and E. Lundstrom, Phys. Rev. D **86**, 075019 (2012) [arXiv:1206.6316 [hep-ph]].
 - [27] CMS Collaboration, Precise determination of the mass of the higgs boson and studies of the compatibility of its couplings with the standard model, Te ch. Rep. CMS-PAS-HIG-14-009, CERN, Geneva, Jul, 2014
 - [28] G. Aad *et al.* [ATLAS Collaboration], Phys. Rev. D **90**, no. 11, 112015 (2014) [arXiv:1408.7084 [hep-ex]].
 - [29] B. A. Kniehl, Nucl. Phys. B **352**, 1 (1991).

- [30] S. Kanemura, Y. Okada, E. Senaha and C.-P. Yuan, Phys. Rev. D **70**, 115002 (2004) [hep-ph/0408364]. S. Kanemura, S. Kiyoura, Y. Okada, E. Senaha and C. P. Yuan, Phys. Lett. B **558**, 157 (2003) [hep-ph/0211308].
- [31] S. Kanemura, M. Kikuchi and K. Yagyu, arXiv:1502.07716 [hep-ph].
- [32] W. Hollik and S. Penaranda, Eur. Phys. J. C **23**, 163 (2002) [hep-ph/0108245]. A. Dobado, M. J. Herrero, W. Hollik and S. Penaranda, Phys. Rev. D **66**, 095016 (2002) [hep-ph/0208014].
- [33] T. Hahn, Comput. Phys. Commun. **140**, 418 (2001); T. Hahn, C. Schappacher, Comput. Phys. Commun. **143**, 54 (2002); T. Hahn and M. Perez-Victoria, Comput. Phys. Commun. **118**, 153 (1999); J. Küblbeck, M. Böhm and A. Denner, Comput. Phys. Commun. **60**, 165 (1990).
- [34] G. J. van Oldenborgh, Comput. Phys. Commun. **66**, 1 (1991); T. Hahn, Acta Phys. Polon. B **30**, 3469 (1999), PoS ACAT **2010**, 078 (2010) [arXiv:1006.2231 [hep-ph]].
- [35] Bohm, H. Spiesberger and W. Hollik, Fortsch. Phys. **34**, 687 (1986). A. Denner, Fortsch. Phys. **41**, 307 (1993) [arXiv:0709.1075 [hep-ph]].
- [36] K. Cheung, J. S. Lee and P. -Y. Tseng, JHEP **1305**, 134 (2013) [arXiv:1302.3794 [hep-ph]]. G. Belanger, B. Dumont, U. Ellwanger, J. F. Gunion and S. Kraml, Phys. Lett. B **723**, 340 (2013) [arXiv:1302.5694 [hep-ph]]. G. Belanger, B. Dumont, U. Ellwanger, J. F. Gunion and S. Kraml, Phys. Rev. D **88**, 075008 (2013) [arXiv:1306.2941 [hep-ph]]. [arXiv:1302.5694 [hep-ph]]. G. Belanger, B. Dumont, U. Ellwanger, J. F. Gunion and S. Kraml, Phys. Rev. D **88**, 075008 (2013) [arXiv:1306.2941 [hep-ph]]. J. R. Espinosa, M. Muhlleitner, C. Grojean and M. Trott, JHEP **1209**, 126 (2012) [arXiv:1205.6790 [hep-ph]]; O. Lebedev, H. M. Lee and Y. Mambrini, Phys. Lett. B **707**, 570 (2012) [arXiv:1111.4482 [hep-ph]]; C. Englert, M. Spannowsky and C. Wymant, Phys. Lett. B **718**, 538 (2012) [arXiv:1209.0494 [hep-ph]].
- [37] G. Belanger, F. Boudjema, J. Fujimoto, T. Ishikawa, T. Kaneko, Y. Kurihara, K. Kato and Y. Shimizu, Phys. Lett. B **576**, 152 (2003) [hep-ph/0309010].
- [38] G. 't Hooft and M. J. G. Veltman, Nucl. Phys. B **44**, 189 (1972). G. 't Hooft and M. J. G. Veltman, Nucl. Phys. B **153**, 365 (1979).
- [39] G. Passarino and M. J. G. Veltman, Nucl. Phys. B **160**, 151 (1979).